

Pitfalls in the Diagnosis of Thoracic Aortic Dissection at CT Angiography¹

Poonam Batra, MD • Brian Bigoni, MD • John Manning, MD • Denise R. Aberle, MD • Kathleen Brown, MD • Eric Hart, MD² • Jonathan Goldin, MD, PhD

Two hundred seventy-five computed tomographic (CT) angiograms of the thoracic aorta were obtained over a period of approximately 4 years in patients with suspected or known aortic dissection. In all cases, unenhanced images were initially obtained, followed by contrast material-enhanced images. A variety of pitfalls were encountered that mimicked aortic dissection. These pitfalls were attributable to technical factors (eg, improper timing of contrast material administration relative to image acquisition); streak artifacts generated by high-attenuation material, high-contrast interfaces, or cardiac motion; periaortic structures (eg, aortic arch branches, mediastinal veins, pericardial recess, thymus, atelectasis, pleural thickening or effusion adjacent to the aorta); aortic wall motion and normal aortic sinuses; aortic variations such as congenital ductus diverticulum and acquired aortic aneurysm with thrombus; and penetrating atherosclerotic ulcer. Although several of these pitfalls are easy to recognize and therefore unlikely to present a diagnostic problem, others are potentially confusing. Familiarity with these common pitfalls, coupled with a knowledge of normal intrathoracic anatomy, will facilitate recognition of true aortic dissection and help avoid misdiagnosis at thoracic aortic CT angiography.

Index terms: Aorta, CT, 94.12916, 94.74 • Aorta, dissection, 94.74, 94.93 • Aortography, 94.121

RadioGraphics 2000; 20:309–320

¹From the Department of Radiological Sciences, UCLA Medical Center, 10833 Le Conte Ave, Los Angeles, CA 90095-1721. Recipient of a Certificate of Merit award for a scientific exhibit at the 1998 RSNA scientific assembly. Received February 26, 1999; revision requested May 17 and received July 1; accepted July 8. **Address reprint requests to** P.B. (e-mail: pbatra@mednet.ucla.edu).

²Current address: Department of Radiology, Northwestern Memorial Hospital, Chicago, Ill.

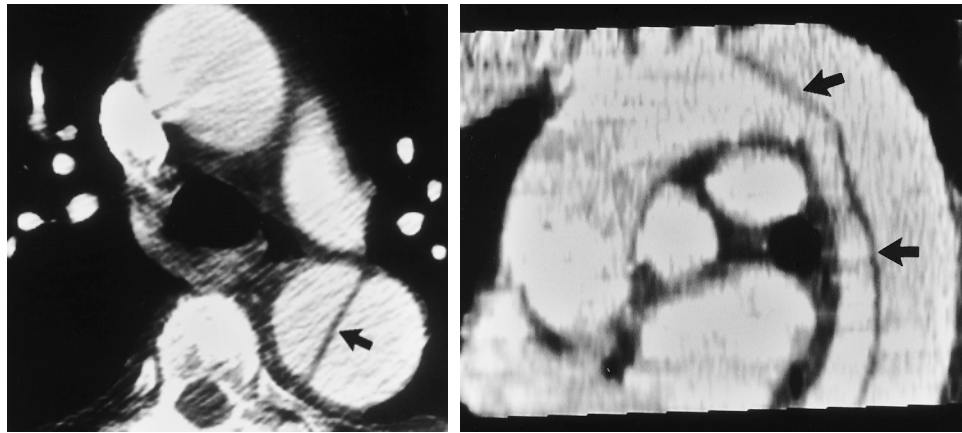


Figure 1. Stanford type B aortic dissection originating immediately distal to the left subclavian artery in an 89-year-old man. **(a)** Axial contrast-enhanced helical CT scan shows a linear area of low attenuation in the descending thoracic aorta (arrow) that represents an intimal flap separating the true and false lumen. **(b)** Sagittal oblique reformatted image of the thoracic aorta demonstrates the intimal flap (arrows) beginning just distal to the origin of the left subclavian artery.

Introduction

Acute aortic dissection is a potentially life-threatening condition that requires prompt and accurate diagnosis to initiate appropriate surgical intervention or medical treatment. Various imaging modalities such as conventional angiography, computed tomography (CT), magnetic resonance (MR) imaging, and multiplanar transesophageal echocardiography are currently available to evaluate patients with suspected or known aortic dissection (1,2). At our institution, thoracic CT angiography is the primary diagnostic imaging technique used to evaluate these patients. Unlike conventional angiography, CT angiography is relatively noninvasive and provides transaxial images rather than projectional images, thus providing superior information about overlapping structures. In addition, CT angiography allows alternative diagnoses by displaying thoracic structures not readily apparent at conventional angiography. Compared with incremental CT, CT angiography can be performed in less time and with better vascular contrast material enhancement. This superior enhancement aids in recognition of an intimal flap, which is a diagnostic feature of aortic dissection. CT angiography, MR imaging, and multiplanar transesophageal echocardiography are equally reliable in the diagnosis of aortic dissection (2).

In this article, we describe our technique of aortic CT angiography and illustrate the spectrum of potential pitfalls that can simulate aortic dissection. We also discuss possible strategies for minimizing false-negative or false-positive diagnosis.

Technique of Aortic CT Angiography

Between August 1994 and November 1998, 275 thoracic CT angiograms were obtained with a helical CT scanner (GE HiSpeed Advantage; GE Medical Systems, Milwaukee, Wisc) or electron beam CT scanner (C-100XL; Imatron, San Francisco, Calif) to evaluate patients with aortic vascular disease. Indications for imaging in patients over 18 years of age included suspected or known aortic dissection (both spontaneous and traumatic) and aortic aneurysms. After a scout view was obtained, initial unenhanced thoracic images were acquired (with respiration suspended whenever possible). These images were obtained from the lung apex to the upper abdomen with 10-mm collimation and a pitch of 1 for helical CT and with 8-mm collimation and 8-mm table incrementation for electron beam CT. Contrast material-enhanced images were obtained from 2 cm above the aortic arch to the diaphragmatic hiatus during intravenous administration of 90–120 mL of nonionic contrast material (iodine, 350 mg/mL) (iohexol [Omnipaque 350; Nycomed, Princeton, NJ]) with an automated power injector at a flow

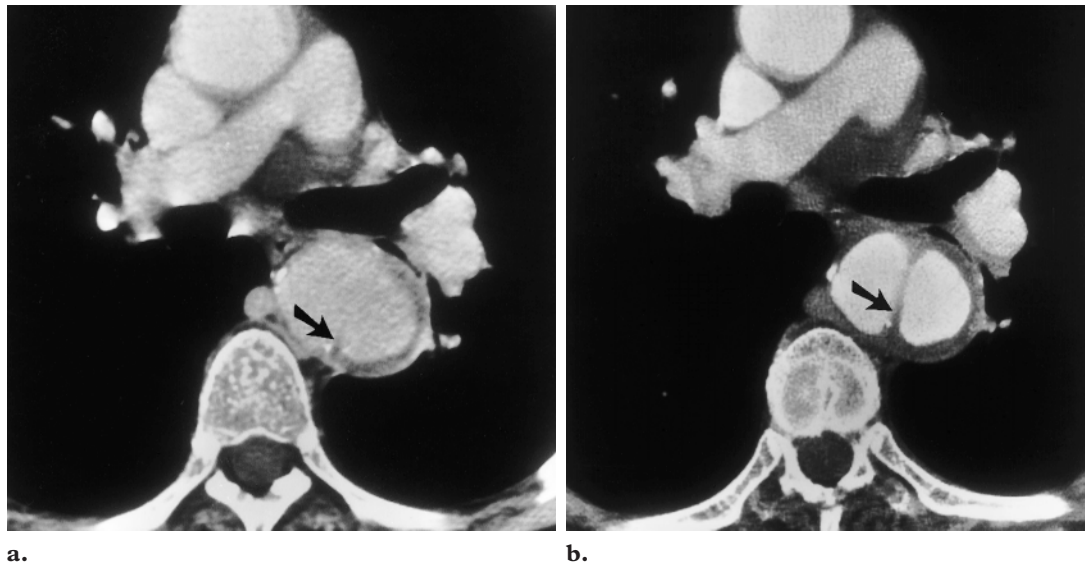


Figure 2. Poor visualization of an intimal flap due to improper timing of contrast material administration. **(a)** Axial contrast-enhanced helical CT scan shows suboptimal aortic enhancement with poor visualization of an intimal flap (arrow), which may result in a false-negative diagnosis. **(b)** On an axial contrast-enhanced helical CT scan obtained with better synchronization of contrast material administration and image acquisition, the intimal flap (arrow) is easily identified in the well-enhanced aorta.

rate of 3 mL/sec with a delay time of 30 seconds. Contrast-enhanced images were obtained at helical CT with 3-mm collimation and a pitch of 1.4–2, and retrospective reconstructed images were obtained at 2-mm intervals. At electron beam CT, images were obtained with a continuous volumetric mode with 3-mm collimation, 2-mm table incrementation, and a scan time of 200–300 msec/section. Two-dimensional reformatted images were obtained in an oblique sagittal plane parallel to the aortic arch in selected cases. Further imaging of the abdominal aorta was performed to demonstrate the full extent of dissection when thoracoabdominal involvement was suspected or detected.

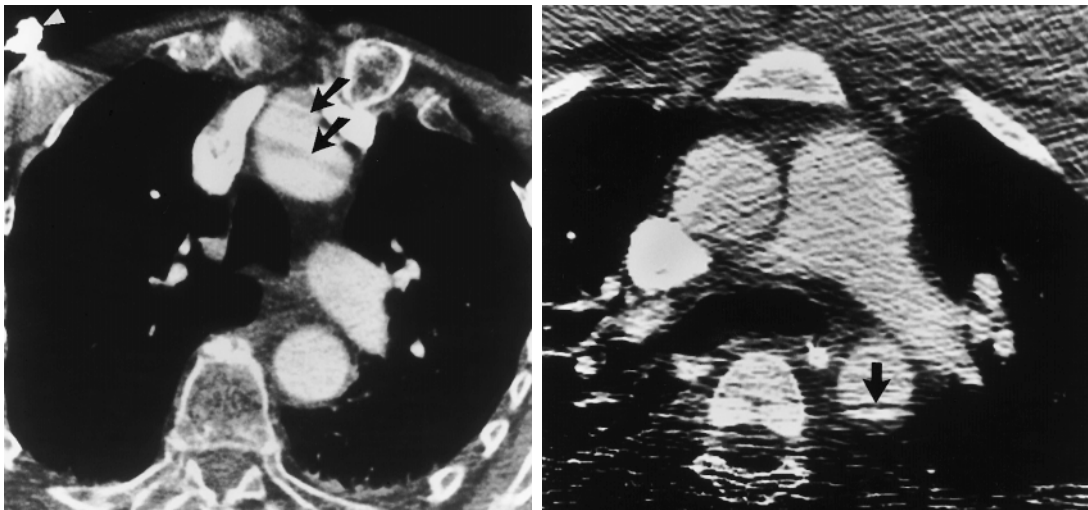
Although a timing scan is not routinely obtained at our institution, it can be obtained in patients with severe cardiac dysfunction to determine the time delay required for peak aortic enhancement (3). In this procedure, 20 mL of contrast material is injected into a peripheral vein at a rate of 3 mL/sec. At helical CT, beginning 10 seconds after the start of injection, 20 dynamic images are obtained at the level of the aortic root at 2-second intervals (ie, 1 sec/section acquisition time, 1-second interscan delay). At electron beam CT, images are obtained with a 100 msec/section acquisition time and a 1-second interscan delay. A time-attenuation curve is generated at the descending thoracic aorta (aortic root level), and delay time is calculated from the start of injection to peak aortic enhancement.

Diagnostic Criteria and Pitfalls

A confident diagnosis of aortic dissection was based on the detection of an intimal flap in the thoracic aorta that separated the true and false lumen (Fig 1). Several artifacts and pitfalls were encountered that could result in false-negative or false-positive diagnosis. These were attributable to (a) technical factors, (b) streak artifacts, (c) periaortic structures (eg, aortic arch branches, mediastinal veins, pericardial recess, thymus, atelectasis, pleural thickening or effusion adjacent to the aorta) (d) aortic wall motion and normal aortic sinuses, (e) aortic variations such as congenital ductus diverticulum and acquired aortic aneurysm with thrombus, and (f) penetrating atherosclerotic ulcer. Many of the artifacts that simulate aortic dissection are suspected due to lack of deformity of the aortic lumen.

Technical Factors

Excellent vascular enhancement is critical to the diagnosis of aortic dissection. Insufficient contrast enhancement of the aortic lumen secondary to improper timing of contrast material administration relative to image acquisition (Fig 2) or a slow rate of injection may not allow sufficient enhancement of the lumen to demonstrate an intimal flap, resulting in false-negative diagnosis.



Figures 3, 4. (3) Streak artifact caused by a pacemaker lead. Axial contrast-enhanced helical CT scan shows two linear areas of low attenuation crossing the ascending aorta and simulating intimal flaps (arrows). These streak artifacts radiate from a pacemaker lead located on the right anterior chest wall (arrowhead). (4) Streak artifact caused by suboptimal arm positioning. Axial contrast-enhanced helical CT scan obtained at the level of the main pulmonary artery demonstrates a horizontal linear area of low attenuation in the descending thoracic aorta simulating an intimal flap (arrow). The patient was unable to elevate his arms and was scanned with his arms at his sides. Beam hardening caused by the arms produced the numerous artifacts seen along the posterior thorax.

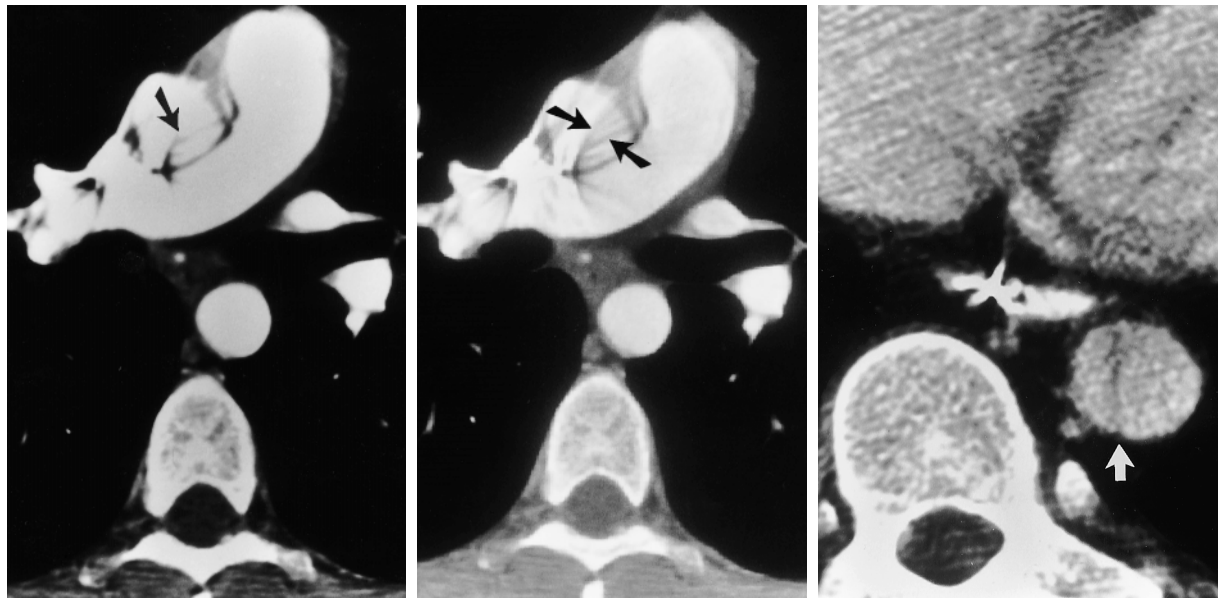
Similarly, in true aortic dissection, an unenhanced false lumen secondary to insufficient scan delay time or delayed contrast enhancement may be misinterpreted as thrombosis of the false lumen (4).

Streak Artifacts

Streak artifacts are generated by high-attenuation material, high-contrast interfaces, and cardiac motion (5). High-attenuation material either within or outside the patient (eg, surgical staples, calcifications, pacemaker leads) may generate streak artifacts (Fig 3). Similarly, if the patient's arms are positioned at the sides during imaging, they may cause beam hardening and produce artifacts (Fig 4). The contrast material in the left brachiocephalic vein or superior vena cava associated with cardiac motion transmitted to these veins may produce artifacts that project over the ascending aorta and the supraaortic arch branches (Fig 5). In addition, the motion of the free wall of the left ventricle may produce artifacts that project over the descending thoracic aorta (Fig 6)

(6). These artifacts are identified on both unenhanced and contrast-enhanced images and are confined to one or two levels. They originate from a high-attenuation structure, appear as straight parallel lines or radiate from a single point, and generally extend beyond the confines of the aorta. Conversely, intimal flaps are characteristically smooth and thin, have a slightly curved appearance, and are restricted to the aortic diameter (7).

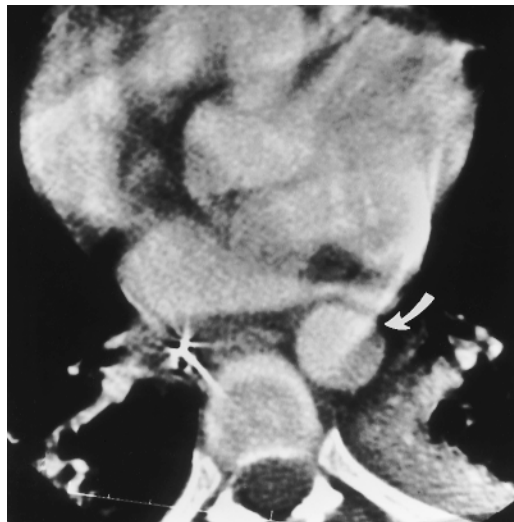
Streak artifacts can be avoided by placing external monitoring devices and the patient's arms outside the scanning field whenever possible. The most problematic streak artifacts originate from an enhanced left brachiocephalic vein and superior vena cava, projecting over the ascending thoracic aorta and simulating Stanford type A dissection. Strategies to minimize these artifacts include the use of diluted contrast material (8), injection of contrast material into a right antecubital vein or lower-extremity vein, and scan acquisition in a caudocranial direction. However, peak aortic enhancement is more unpredictable with pedal injection than with antecubital injection (4). Streak artifacts, particularly the extraortic



5a.

5b.

6a.



6b.

Figures 5, 6. (5) Streak artifact caused by contrast material in the right pulmonary artery. (a) Axial contrast-enhanced helical CT scan obtained at the level of the main pulmonary artery demonstrates a semilunar streak artifact along the posterior aspect of the ascending thoracic aorta simulating an intimal flap (arrow). (b) Axial contrast-enhanced helical CT scan obtained with optimal window width and level settings better demonstrates the aortic lumen and wall. Multiple streak artifacts are also more readily seen (arrows). (6) Streak artifact caused by cardiac motion. (a) Axial contrast-enhanced helical CT scan shows a linear area of low attenuation in the descending thoracic aorta simulating an intimal flap (arrow). This artifact was not present on adjacent sections (not shown). (b) Axial contrast-enhanced helical CT scan obtained in a different patient shows a streak artifact in the descending aorta (arrow) resembling differential filling of the true and false lumen seen in aortic dissection. High-contrast interfaces between left ventricular wall motion and the adjacent lung generate artifacts that project across the descending aorta and may simulate an intimal flap or double lumina.

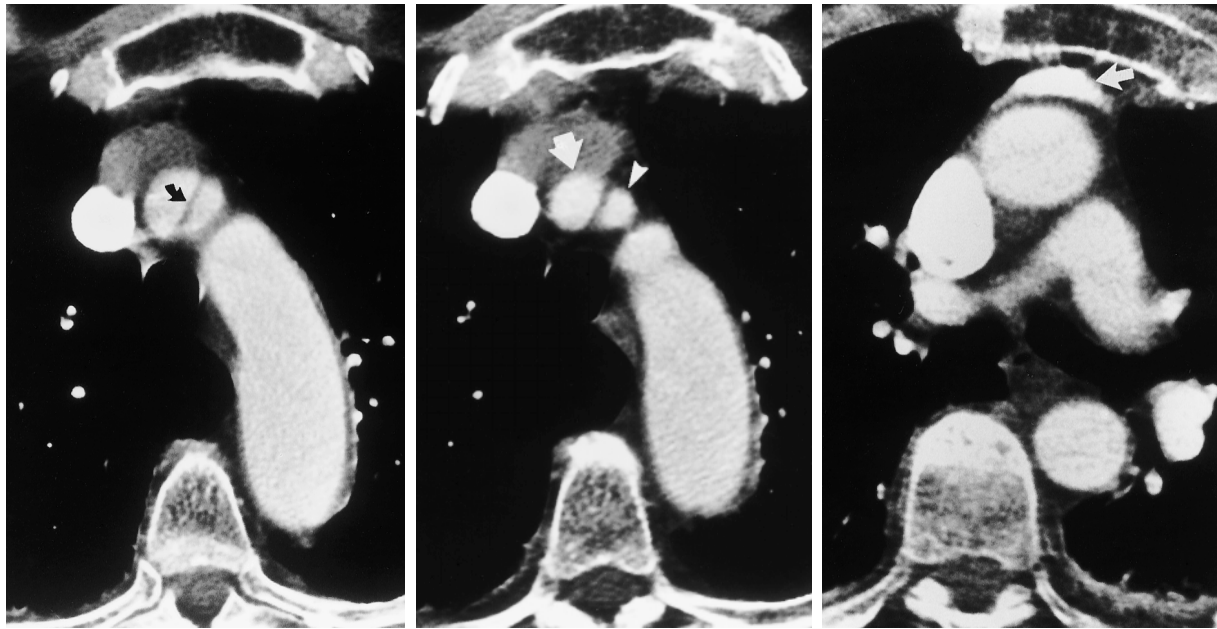
extension of these artifacts, can be better visualized by optimizing window width and level settings on a console (7).

Periaortic Structures

Several periaortic vascular structures such as the origin of the aortic arch vessels and the left brachiocephalic, superior intercostal, and pulmonary veins may be misinterpreted as double lumina or intimal flaps. Similarly, superior pericardial recess, residual thymus, atelectasis, pleural thickening, or pleural effusion adjacent to the thoracic aorta may also be misinterpreted as aortic dissec-

tion. Focal periaortic soft-tissue masses such as periaortic fibrosis or lymphoma may be difficult to distinguish from aortic dissection. These periaortic masses have irregular external margins compared with the intramural hematoma seen in aortic dissection, which has a smooth, crescentic appearance (9).

The origin of the aortic arch arteries may mimic aortic dissection. The walls of the adjacent arterial branches may simulate an intimal flap but can be identified on subsequent images (Fig 7).

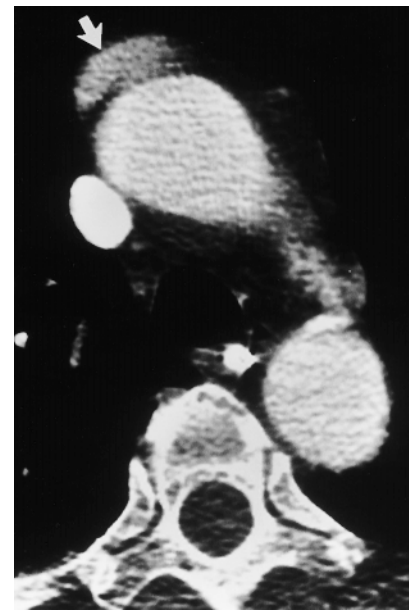


7a.

7b.

8.

Figures 7–9. (7) Origins of the brachiocephalic artery and left common carotid artery mimicking dissection. (a) Axial contrast-enhanced CT scan shows a linear area of low attenuation in a great vessel adjacent to the aortic arch simulating an intimal flap (arrow). (b) Contrast-enhanced CT scan obtained cephalad to a shows that this area represents the walls of the brachiocephalic (arrow) and left common carotid (arrowhead) arteries originating from the aortic arch. (8) Left brachiocephalic vein simulating aortic dissection. Axial contrast-enhanced electron beam CT scan obtained at the level of the left pulmonary artery demonstrates a semilunar area of high attenuation anterior to the ascending aorta (arrow). The normal aortic wall between the left brachiocephalic vein and the ascending thoracic aorta simulates an intimal flap. Note that the left brachiocephalic vein is isoattenuating relative to the superior vena cava and hyperattenuating relative to the aorta. The contrast material was administered via a left antecubital vein. (9) Left brachiocephalic vein mimicking aortic dissection. Axial contrast-enhanced helical CT scan demonstrates a curvilinear area of low attenuation anterior to the ascending aorta (arrow), which adjacent sections (not shown) helped confirm as a low-positioned brachiocephalic vein. The contrast material was administered via a right antecubital vein; consequently, the unenhanced left brachiocephalic vein could be misinterpreted as a false lumen.



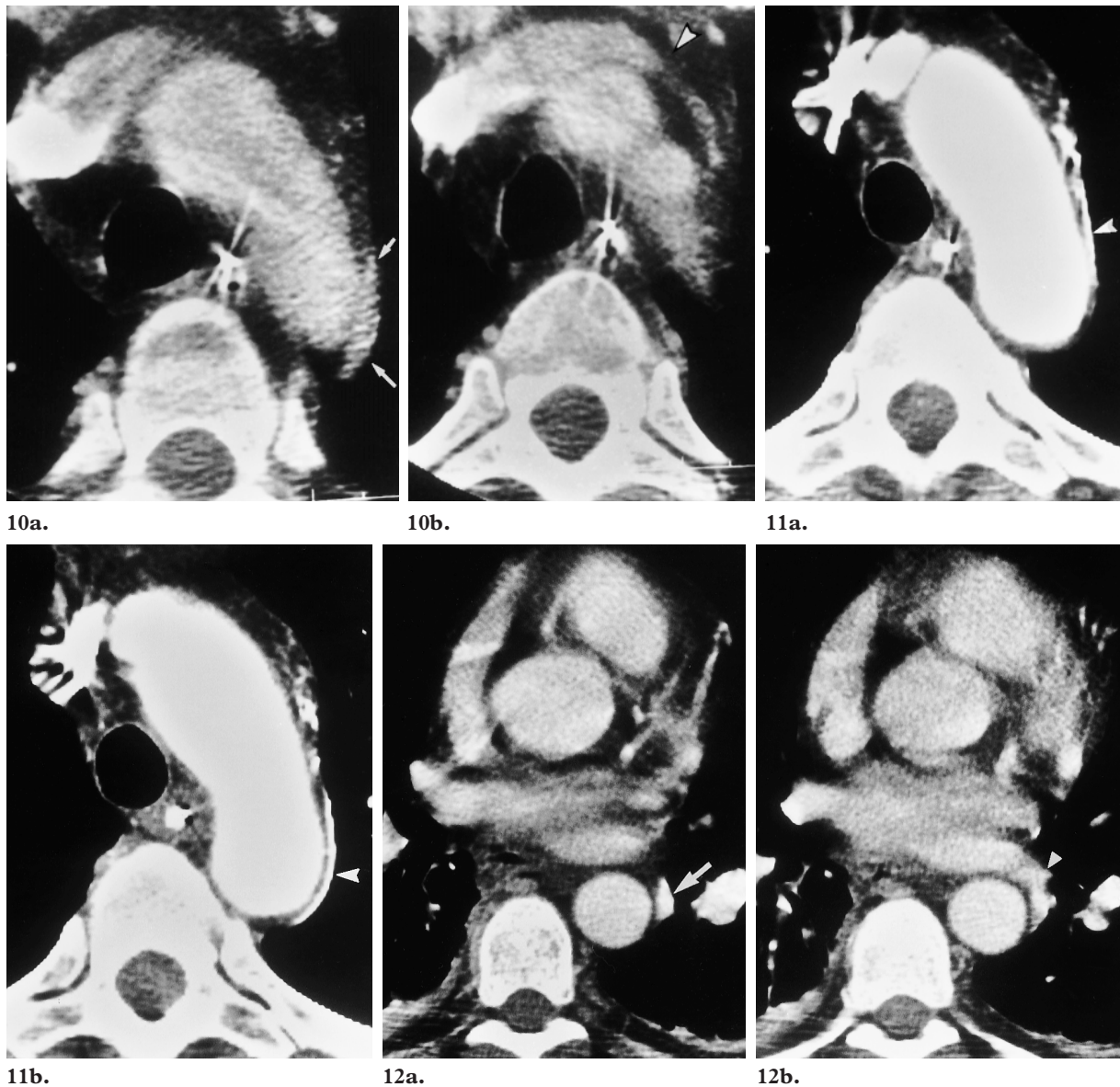
9.

The left brachiocephalic vein usually courses anterior to the supraaortic branches of the aortic arch. In some cases, when it is low-lying, it may pass anterior to the aortic arch itself and be misinterpreted as aortic dissection (Figs 8, 9) (10).

The left superior intercostal vein normally abuts the aortic arch as it passes from the accessory hemiazygos vein posteriorly to the left brachiocephalic vein anteriorly and may resemble a contrast material–filled double aortic lumen. Knowledge of the normal anatomy of this vessel

and recognition of the vessel on contiguous images can help avoid this interpretive error (Figs 10, 11).

The left inferior pulmonary vein may be juxtaposed with the descending thoracic aorta and can mimic a double lumen of dissection (Fig 12). This pitfall usually occurs when the left atrium is enlarged (6). The continuity of the vein with the left atrium centrally and its branching pattern in the lung peripherally on adjacent sections can help make the necessary distinction.



Figures 10–12. (10) Left superior intercostal vein mimicking a double lumen. (a) Axial contrast-enhanced helical CT scan demonstrates an enhancing structure alongside the aortic arch simulating aortic dissection (arrows). (b) On an axial contrast-enhanced helical CT scan obtained cephalad to a, the structure is seen terminating in the left brachiocephalic vein (arrowhead), a finding that confirms the structure to be the left superior intercostal vein. (11) Left superior intercostal vein mimicking a double lumen. Adjacent axial contrast-enhanced helical CT scans obtained at the level of the aortic arch demonstrate an enhancing structure lateral to the aortic arch in the expected location of the left superior intercostal vein (arrowhead). (12) Left inferior pulmonary vein simulating a double lumen. (a) Axial contrast-enhanced helical CT scan obtained at the level of the left atrium demonstrates a curvilinear area of high attenuation lateral to the descending aorta (arrow). (b) Axial contrast-enhanced helical CT scan obtained cephalad to a reveals that this high-attenuation area is contiguous with the left inferior pulmonary vein (arrowhead).

Superior pericardial recess can be misinterpreted as Stanford type A dissection. The retro-aortic portion of a superior pericardial recess forms a semilunar area along the right posterior wall of the ascending thoracic aorta, whereas the preaortic portion is seen anterior to the ascending

aorta. These recesses occur just above or at the level of the left pulmonary artery and can be recognized by their water attenuation, focal nature, and typical anatomic location (Fig 13). The

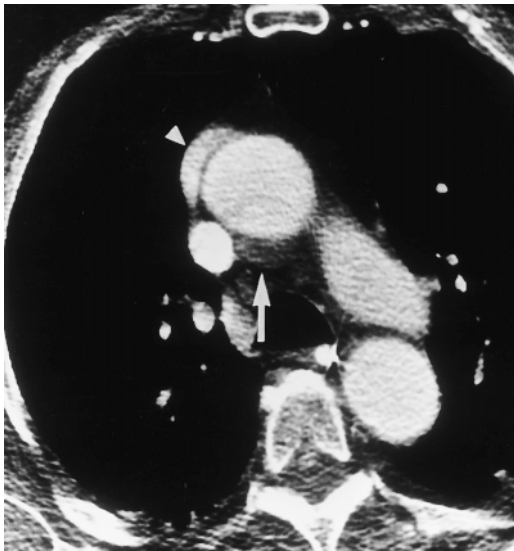


Figure 13. Superior pericardial recess mimicking aortic dissection. Axial contrast-enhanced helical CT scan shows a semilunar area of low attenuation abutting the posterior aspect of the ascending thoracic aorta (arrow), a finding that can be misinterpreted as a false lumen. Note also the crescentic area of high attenuation representing the left brachiocephalic vein coursing anterolateral to the ascending thoracic aorta and mimicking dissection (arrowhead).

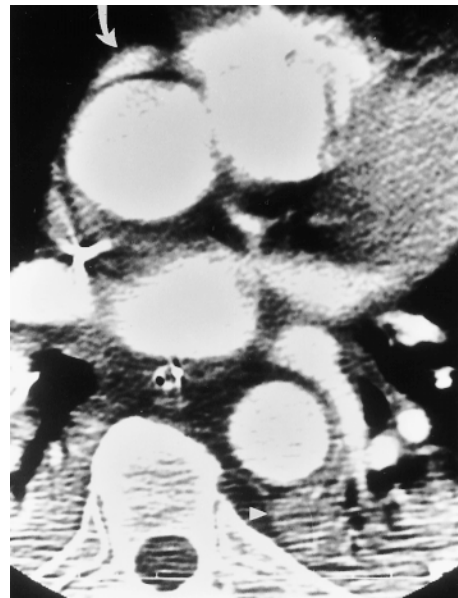


Figure 14. Right atrial appendage simulating aortic dissection. Axial contrast-enhanced helical CT scan obtained near the aortic root demonstrates a crescentic enhancing structure anterior to the aorta (arrow) simulating the double aortic lumina seen in dissection. CT scans obtained more caudad (not shown) revealed this structure to be a right atrial appendage contiguous with the right atrium. Note also the atelectasis in the left lower lobe adjacent to the descending thoracic aorta (arrowhead).

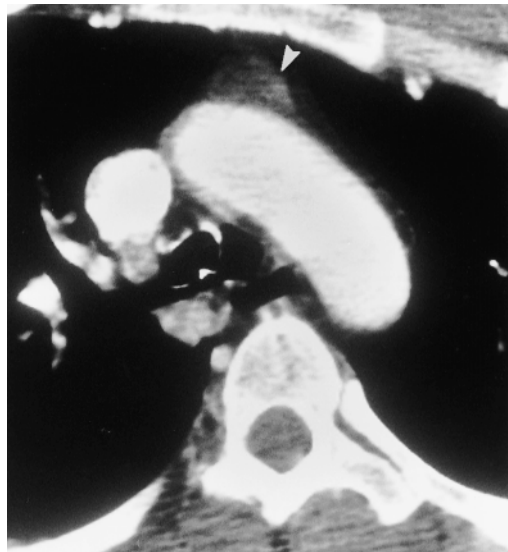
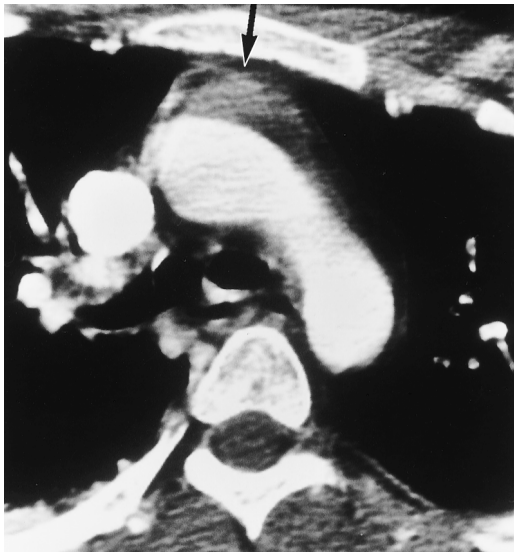
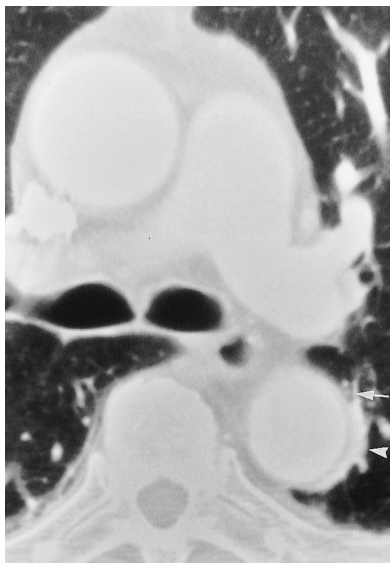


Figure 15. Residual thymus mimicking a false lumen. **(a)** Axial contrast-enhanced helical CT scan obtained at the level of the aortic arch demonstrates an area of soft-tissue attenuation anterior to the aorta (arrow), a finding that can be misinterpreted as a false lumen. **(b)** Axial contrast-enhanced helical CT scan obtained cephalad to **(a)** demonstrates the triangular configuration of this finding (arrowhead), which is consistent with residual thymus given the young age of the patient.



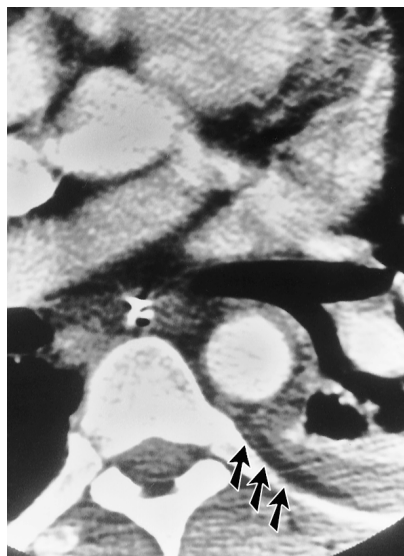
16a.



16b.



17a.



17b.

Figures 16, 17. (16) Atelectasis mimicking Stanford type B dissection. (a) Axial contrast-enhanced helical CT scan obtained at the level of the main pulmonary artery demonstrates a crescentic area of enhancement posterolateral to the descending thoracic aorta (arrowhead). The normal aortic wall between the contrast material-filled aortic lumen and the atelectatic lung is seen as a thin linear area of low attenuation resembling an intimal flap (arrow). A similar appearance results when thickened pleura abuts the descending thoracic aorta. (b) Axial contrast-enhanced helical CT scan obtained with lung windowing helps confirm the presence of atelectasis in the left lower lobe (arrowhead). Note that a subsegmental bronchus leads into the atelectatic lung, producing an air bronchogram (arrow). (17) Pleural effusion simulating aortic dissection. (a) Axial contrast-enhanced helical CT scan obtained at the level of the midheart demonstrates a region of low attenuation along the left lateral aspect of the descending thoracic aorta simulating a false lumen (arrow). Note also the atelectasis in the left lower lobe (*). (b) Axial contrast-enhanced helical CT scan obtained cephalad to a at the level of the aortic root shows this low-attenuation region to be contiguous with pleural fluid (arrows), a finding that confirms the presence of pleural effusion.

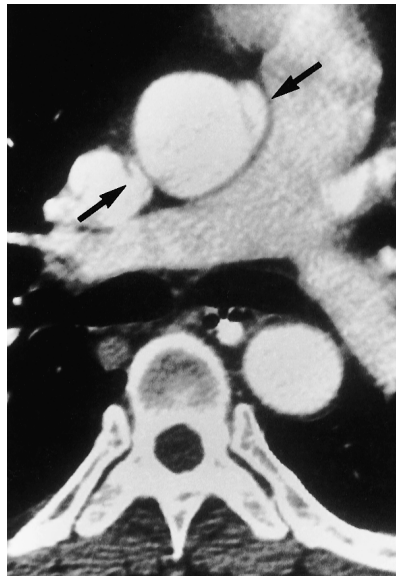
presence of hemopericardium increases the CT attenuation of a recess (11). Thickened pericardium anterior to the ascending aorta can also simulate a double lumen, but the presence of thickened pericardium at other levels can help avoid misinterpretation. The right arterial appendage may extend anteriorly to abut the ascending aorta and mimic a false lumen (Fig 14). However, its continuity with the right atrium on adjacent sections can help prevent a false-positive diagnosis.

In young patients, residual thymus located anterior to the ascending thoracic aorta may resemble a double lumen (Fig 15). The triangular configuration of residual thymus and its confinement to the anterior mediastinum along with the young age of the patient can help avoid misinterpretation.

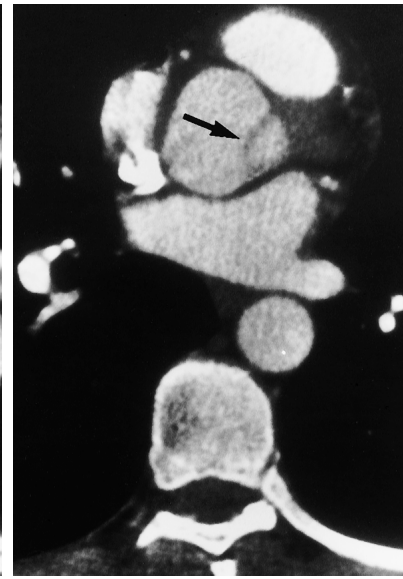
Atelectasis, pleural thickening, or pleural effusion adjacent to the descending thoracic aorta may resemble a false lumen. Contrast-enhanced atelectatic lung may resemble a false lumen, whereas the normal aortic wall between the contrast material-filled aorta and atelectatic lung may simulate an intimal flap (Fig 16). Atelectatic lung can be recognized by reviewing images with lung windowing because it often contains some air (5) or produces air bronchograms. Pleural effusion appears as a low-attenuation region adjacent to the descending thoracic aorta and can be recognized by its contiguity with the pleural fluid on adjacent sections (Fig 17).



18a.



18b.

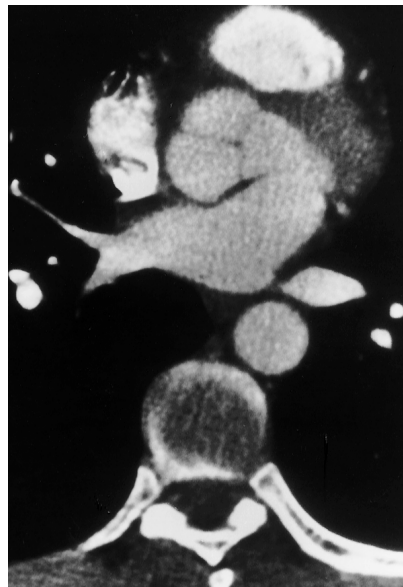


19a.

Figures 18, 19. (18) Aortic motion artifact simulating aortic dissection. (a) Axial contrast-enhanced helical CT scan obtained at the aortic root shows a curvilinear area of low attenuation along the left anterior and right posterior aspects of the ascending aorta (arrows). (b) Axial contrast-enhanced helical CT scan obtained at the aortic root in a different patient demonstrates a low-attenuation interface along the left and right lateral aspects of the aorta simulating an intimal flap (arrows). (19) Aortic valve cusps simulating intimal flaps. (a) Axial contrast-enhanced electron beam CT scan shows a curvilinear area of low attenuation along the left lateral aspect of the aortic root simulating an intimal flap (arrow). (b) Axial contrast-enhanced electron beam CT scan obtained caudad to a reveals that the low-attenuation area does not represent an intimal flap but the semilunar cusp of the aortic valve.

Aortic Wall Motion and Normal Aortic Sinuses

Aortic wall motion during cardiac systole and diastole produces curvilinear artifacts in the proximal ascending aorta that are most pronounced at the aortic root. In the majority of cases, the artifacts occur at the left anterior and right posterior aspects of the aortic circumference. The position of the artifacts is related to the pendular motion of the ascending aorta, which on axial scans demonstrates a position on the aortic circumference between 12 or 1 o'clock and 6 or 7 o'clock (12). Occasionally, the artifact appears as a circle overlying the circumference of the ascending aorta (13). This appearance may be related to combined pendular and circular motion of the ascending aorta (12). The motion artifact can be recognized by its characteristic location at the aortic root and its restriction to only one or two adjacent sections (Fig 18). The artifact can be minimized with reconstructed images obtained with a 180° linear-interpolation algorithm (14).



19b.

It may also be reduced by obtaining images with ultrafast electron beam CT. Images of the ascending aorta can be further improved with electrocardiographic triggering at electron beam CT (15).

The normal aortic sinuses of Valsalva may simulate an intimal flap at the aortic root but can be recognized by their location (Fig 19). The sinuses are visualized at the same level as the proximal left coronary artery (16).

Congenital Aortic Diverticulum and Acquired Aortic Aneurysm

Aortic diverticulum typically occurs at the aortic isthmus and manifests as a smooth, focal bulge that forms obtuse angles with the aortic wall. It is

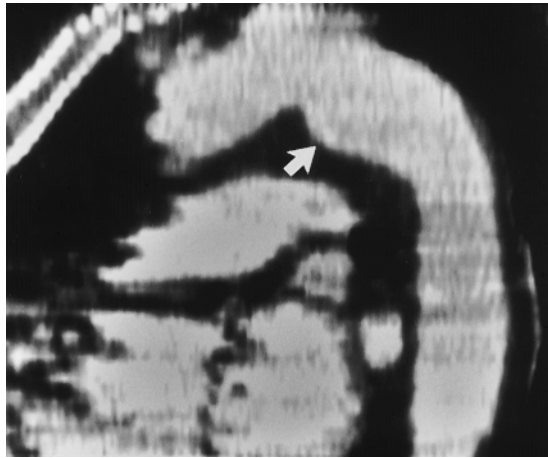


Figure 20. Ductus diverticulum simulating aortic dissection. Sagittal oblique reformatted CT scan demonstrates a focal bulge at the anteromedial aspect of the aortic isthmus. Note the smooth margins and the typical gentle obtuse angles formed by the ductus diverticulum and the aortic wall (arrow). The diverticulum was difficult to diagnose on axial CT scans. In contrast, false aneurysms occurring with aortic dissection are of variable size and shape, have sharp margins, and often contain an intimal flap.

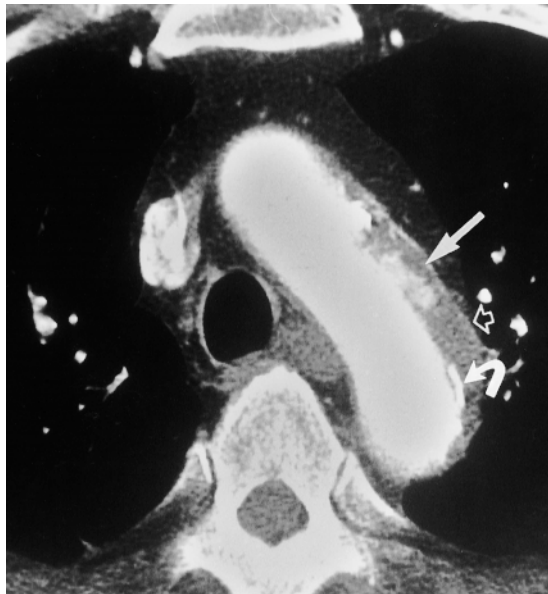


Figure 22. Atherosclerotic penetrating ulcer. Axial contrast-enhanced helical CT scan shows an atherosclerotic ulcer (straight solid arrow) surrounded by intramural hematoma (open arrow) beneath the calcified intima (curved solid arrow).

usually located at the anteromedial aspect of the aorta (Fig 20). False-positive diagnosis may occur if the diverticulum forms an acute superior angle with the aortic wall, has folded back against the aortic wall (thereby simulating an intimal flap), or is atypically located at the anterolateral aspect of the aorta (17).



Figure 21. Aneurysmal dilatation of the aorta with intraluminal thrombus. Axial contrast-enhanced helical CT scan obtained at the level of the aortic arch demonstrates a mildly dilated, enhanced, atherosclerotic aorta containing an intraluminal thrombus. Note the dense calcification at the periphery of the aorta (arrowhead); in true dissection, calcification is inwardly displaced.

A fusiform aortic aneurysm with intraluminal thrombus is often difficult to distinguish from aortic dissection with a thrombosed false lumen. Medial displacement of intimal calcification and a high-attenuation thrombosed false lumen at unenhanced CT suggest the diagnosis of dissection. An aortic aneurysm typically demonstrates peripheral calcification (Fig 21) (18). Furthermore, aneurysms are more often focal, whereas in dissection a long segment of the aorta is typically involved and the thrombosed false lumen spirals around the true lumen (16). A false-positive diagnosis of dissection can occur if there is calcification on the surface of an intraluminal thrombus in an aneurysm. A false-negative diagnosis can occur in patients with chronic aortic dissection who demonstrate peripheral calcification simulating an atherosclerotic aneurysm (19).

Penetrating Atherosclerotic Ulcer

Penetrating atherosclerotic ulcer is an atheromatous lesion that penetrates the internal elastic lamina and extends into the media, resulting in intramural hemorrhage (20). Penetrating ulcer typically appears as a small, focal, contrast material-filled outpouching surrounded by an intramural hematoma (Fig 22). The angiographic

appearance of penetrating ulcer is similar to that of a peptic ulcer at barium radiography (21). The atherosclerotic intimal calcification is displaced inward by the hematoma, and the peripheral aortic wall may demonstrate thickening and contrast enhancement. Penetrating ulcer is more frequently seen in the middle and distal third of the descending thoracic aorta, whereas aortic dissection begins from a tear in the ascending thoracic aorta in approximately two-thirds of cases. In addition, an intimal flap is not present in penetrating ulcer (22). It is important to distinguish penetrating atherosclerotic ulcer from Stanford Type B dissection that occurs just distal to the left subclavian artery because surgical management, if indicated, is more extensive for atherosclerotic ulcer than for aortic dissection (20).

Conclusions

CT angiography of the thoracic aorta is currently the imaging technique of choice at our institution for evaluating patients with suspected or known aortic dissection. Although several of the various pitfalls and artifacts that mimic aortic dissection at CT angiography are easy to recognize and are not likely to present a diagnostic problem, others are potentially confusing. Familiarity with these common pitfalls, coupled with a knowledge of normal intrathoracic anatomy, can help radiologists avoid interpretive errors in the diagnosis of aortic dissection in almost all cases.

References

1. Cigarroa JE, Isselbacher EM, DeSanctis RW, Eagle KA. Diagnostic imaging in the evaluation of suspected aortic dissection. *N Engl J Med* 1993; 328: 35-43.
2. Sommer T, Fehske W, Holzkecht N, et al. Aortic dissection: a comparative study of diagnosis with spiral CT, multiplanar transesophageal echocardiography, and MR imaging. *Radiology* 1996; 199: 347-352.
3. Rubin GD. Helical CT angiography of the thoracic aorta. *J Thorac Imaging* 1997; 12:128-149.
4. Chung JW, Park JH, Im JG, Chung MJ, Han MC, Ahn H. Spiral CT angiography of the thoracic aorta. *RadioGraphics* 1996; 16:811-824.
5. Demos TC, Posniak HV, Marsan RE. CT of aortic dissection. *Semin Roentgenol* 1989; 24:22-37.
6. Godwin JD, Breiman RS, Speckman JM. Problems and pitfalls in the evaluation of thoracic aortic dissection by computed tomography. *J Comput Assist Tomogr* 1982; 6:750-756.
7. Gallagher S, Dixon AK. Streak artifacts of the thoracic aorta: pseudodissection. *J Comput Assist Tomogr* 1984; 8:688-693.
8. Rubin GD, Lane MJ, Bloch DA, Leung AN. Optimization of thoracic spiral CT: effects of iodinated contrast medium concentration. *Radiology* 1996; 201:785-791.
9. Sebastia C, Pallisa E, Quiroga S, Alvarez-Castells A, Dominguez R, Evangelista A. Aortic dissection: diagnosis and follow-up with helical CT. *RadioGraphics* 1999; 19:45-60.
10. Taber P, Chang LWM, Campion GM. The left brachiocephalic vein simulating aortic dissection on computed tomography. *J Comput Assist Tomogr* 1979; 3:360-361.
11. Chiles C, Baker ME, Silverman PM. Superior pericardial recess simulating aortic dissection on computed tomography. *J Comput Assist Tomogr* 1986; 10:421-423.
12. Duvernoy O, Coulden R, Ytterberg C. Aortic motion: a potential pitfall in CT imaging of dissection in the ascending aorta. *J Comput Assist Tomogr* 1995; 19:569-572.
13. Burns MA, Molina PL, Gutierrez FR, Sagel SS. Motion artifact simulating aortic dissection on CT. *AJR Am J Roentgenol* 1991; 157:465-467.
14. Loubeyre P, Angelie E, Grozel F, Abidi H, Minh VAT. Spiral CT artifact that simulates aortic dissection: image reconstruction with use of 180° and 360° linear-interpolation algorithms. *Radiology* 1997; 205:153-157.
15. Nakanishi T, Fukuoka H, Azuma K, Ito K. Electron-beam CT angiography for thoracic aortic aneurysm and dissection: application of continuous volume scan and electrocardiographically triggered scan. *Radiat Med* 1997; 15:155-161.
16. Thorsen MK, Lawson TL, Foley WD. CT of aortic dissections. *CRC Crit Rev Diagn Imaging* 1985; 26:291-324.
17. Morse SS, Glickman MG, Greenwood LH, et al. Traumatic aortic rupture: false-positive aortographic diagnosis due to atypical ductus diverticulum. *AJR Am J Roentgenol* 1988; 150:793-796.
18. Heiberg E, Wolverson MK, Sundaram M, Shields JB. CT characteristics of aortic atherosclerotic aneurysm versus aortic dissection. *J Comput Assist Tomogr* 1985; 9:78-83.
19. Hachiya J, Nitatori T, Yoshino A, Okada M, Furuya Y. CT of calcified chronic aortic dissection simulating atherosclerotic aneurysm. *J Comput Assist Tomogr* 1993; 17:374-378.
20. Stanson AW, Kazmier FJ, Hollier LH, et al. Penetrating atherosclerotic ulcers of the thoracic aorta: natural history and clinicopathologic correlations. *Ann Vasc Surg* 1986; 1:15-23.
21. Hussain S, Glover JL, Bree R, Bendick PJ. Penetrating atherosclerotic ulcers of the thoracic aorta. *J Vasc Surg* 1989; 9:710-717.
22. Kazerooni EA, Bree RL, Williams DM. Penetrating atherosclerotic ulcers of the descending thoracic aorta: evaluation with CT and distinction from aortic dissection. *Radiology* 1992; 183:759-765.